Proceedings of the 10th International Conference on Fluid Flow, Heat and Mass Transfer (FFHMT'23)
Ottawa, Canada – June 07-09, 2023
Paper No. 174
DOI: 10.11159/ffhmt23.174

Thermal-Hydraulic Behaviour Comparison of Two Novel Lattice Structures with Simple Cubic BCC Lattice Structure

Abhishek Dey[1], V. Raghavan[2], G. Venkatarathnam[2]
[1,2]Indian Institute of Technology Madras
IIT P.O., Chennai 600036, India
me20s018@smail.iitm.ac.in; raghavan@iitm.ac.in
gvenkat@iitm.ac.in

Abstract – Additively manufactured lattice structures have the potential to replace traditional fins in heat exchangers. In this study, two new lattice structures with different strut diameters are modelled (namely TYPE-A, TYPE-B, TYPE-C, TYPE-D) and numerically compared with a simple cubic BCC (SC-BCC) lattice structure. The results show that all the lattice structures outperform SC- BCC lattice structure in terms of heat transfer. However, they also exhibit a higher pressure drop than SC-BCC lattice. Although the TYPE-A lattice has the highest lattice heat transfer coefficient, due to its lower fin efficiency, it exhibits less heat transfer than the TYPE-D lattice. TYPE-B lattice, which is a modified version of the TYPE-A lattice, shows less heat transfer and pressure drop. To identify the lattice structure with the best thermal-hydraulic behaviour, area goodness factor of each lattice structure is evaluated. The results reveal that TYPE-A lattice has an area goodness factor almost 50% higher than the SC-BCC lattice. This indicates that TYPE-A lattice structure is better suited for heat transfer applications where high heat transfer is required.

***Keywords*:** Heat Exchanger, Computational Fluid Dynamics, Additive Manufacturing, Lattice Structure, Heat Transfer

1. Introduction

Heat exchangers play a crucial role in many engineering applications, including power generation, chemical processing, and refrigeration systems. The transfer of heat between fluids is a critical process that affects the overall efficiency and performance of these systems. As a result, researchers have been studying ways to improve heat transfer between fluids in heat exchangers for several decades. Various types of fins, such as louvered, wavy and offset strip fins, have been developed and extensively studied to enhance heat transfer. These fins or secondary surfaces increase the surface area density of the heat exchanger, reducing thermal resistance and enhancing heat transfer. However, traditional fin designs have limitations in terms of their surface area density (surface area per unit volume) and ability to mix fluids efficiently.

Recent advancements in manufacturing technology, such as 3D printing, have made it possible to produce complex lattice structures that were previously impossible to manufacture using conventional methods. Higher surface area density and higher fluid mixing rate make lattice structures suitable for replacing conventional fins in heat exchangers.

Dixit et al. [1] conducted a numerical comparison of various lattice structures based on their thermal and hydraulic behaviour. Despite having lower surface area density, simple cubic and simple cubic BCC structures were found to exhibit superior thermal-hydraulic behaviour compared to other lattice structures. Takarazawa et al. [2] also evaluated a numerical comparison of various lattice structures for their thermal-hydraulic behaviour and experimentally verified the results. They observed that although FCC had a higher surface area density, both BCC and BCCZ lattice structures exhibited superior thermal performance. Yun et al. [3] experimentally validated a FCCZ lattice structure performance and performed a thermal-structural analysis to find the best porosity level. Wong et al. [4] conducted experiments to assess the effectiveness of a 3D printed lattice as aluminium heat sink compared to conventional pin-fin and rectangular-fin heat sinks. Despite having a higher surface area density, the lattice structures showed a lower heat transfer rate. This could be due to bypassing of the flow through the lattice structure. Liang et al. [5] compared different lattices and concluded that heat transfer enhancement strongly depends on the vortex generated in the fluid. Kumar et al. [6] studied the effect of orientation of a hexagonal periodic cellular structure, and the results showed that changing the orientation had a significant impact on both heat transfer and pressure drop values. Xinhuan et al. [7] manufactured a BCC lattice integrated tube heat exchanger and evaluated its

performance against a smooth tube while circulating supercritical CO_2. Their results revealed an improvement in heat transfer with the BCC lattice structure.

The available literature reveals that, although FCC possesses a high surface area density, its heat transfer coefficient is considerably lower than that of the BCC lattice due to fluid flow bypassing. Therefore, there is a need for a novel lattice structure that simultaneously offers a high heat transfer coefficient and surface area density. In this study, two novel lattice structures are developed and compared with the existing Simple Cubic BCC (SC-BCC) lattice structure.

2. Numerical Methodology

2.1. Model

Two novel lattice structures are modelled and evaluated alongside the conventional SC-BCC lattice within the same simulation domain with same Reynolds number to compare their thermal-hydraulic behaviour. The corresponding lattice configurations are presented in Fig. 1, where Fig. 1a displays the SC-BCC lattice, Fig. 1b represents the TYPE-A lattice, and Fig. 1c showcases the TYPE-B, TYPE-C and TYPE-D lattices with varying strut diameters. The porosity (ratio of fluid volume and total volume) of SC-BCC, TYPE-A, and TYPE-C lattices are identical at 77%, while TYPE-B lattice has the same strut diameter as TYPE-A lattice at 0.483 mm, and TYPE-D lattice has the same strut diameter as SC-BCC lattice at 0.677 mm. TYPE-C lattice, on the other hand, has a strut diameter of 0.515 mm.

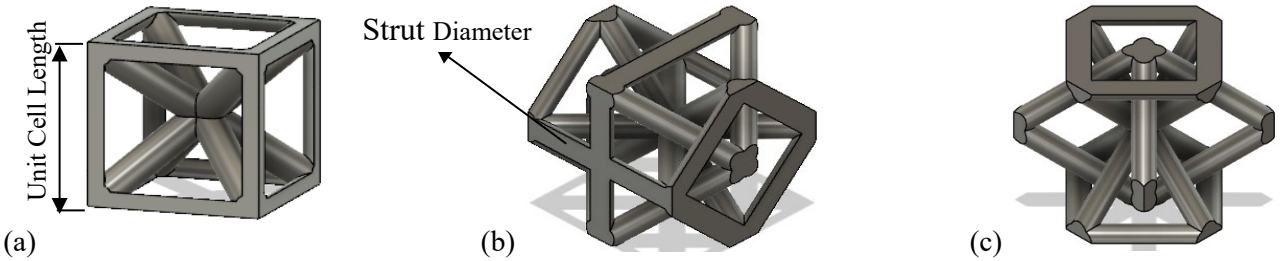

Fig. 1: (a) Simple Cubic BCC lattice structure, (b) TYPE-A lattice structure and (c) TYPE-B, TYPE-C and TYPE-D lattice structure

2.2. Computational Domain and Boundary Conditions

The computational domain consists of seven lattices along the flow length, with an extension region of 7 mm provided before and after the lattice structure to prevent convergence-related issues arising from backflow. Each lattice has a unit cell length of 3.5 mm, and a 0.5 mm thick solid plate is attached below the lattice. To decrease computational costs, only one lattice has been utilised in the transverse direction of the flow.

Boundary conditions for the simulation domain are illustrated in Fig. 2. A constant velocity with a temperature of 20º C is provided at the inlet, and a pressure outlet boundary condition is applied at the outlet. Symmetry-type boundary conditions are applied to the sides. The top is insulated along with no-slip boundary condition for velocity. The bottom wall is maintained at a constant temperature of 75º C. The bottom of the fluid domain is assigned a no-slip velocity boundary condition and an insulated temperature boundary condition. All other boundaries of the solid domain are specified as insulated. The fluid domain consists of air, while SS304 stainless steel is selected as the solid domain.

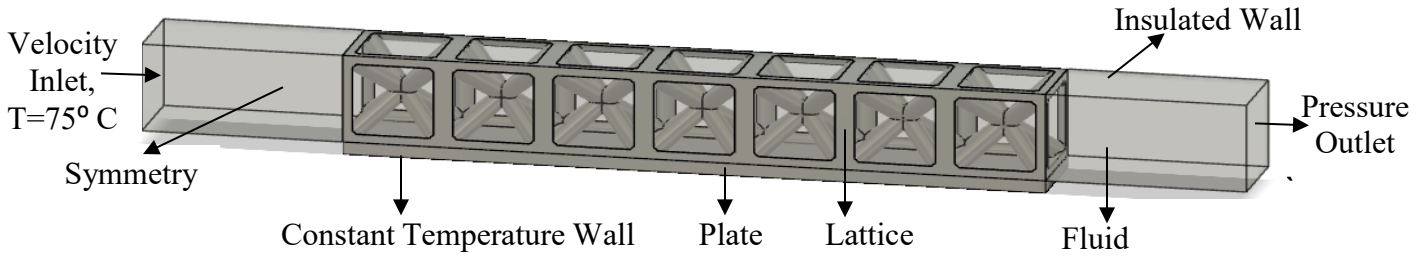

Fig. 2: Computational domain and Boundary Conditions of SC-BCC lattice structure

2.4. Solver Validation and Grid Independence Study

The 'chtMultiRegionFoam' solver is called from OpenFOAM software to numerically simulate the domain. SIMPLE SIMPLE algorithm with a second-order upwind scheme is used to solve continuity, momentum and energy equations with with $k-\omega\ SST$ turbulence model. Solver validation is done with Sungho et al. [3] paper, and a maximum of 14% error in in pressure drop and 5% for temperature is recorded with their experimental results for higher Reynolds number.

Solid, lattice and fluid domains are discretised into complete tetrahedral cells using the Salome software. To ensure a mesh-independent response, a mesh convergence analysis is performed to determine the minimum number of cells required. Depending on the lattice geometries, the number of cells required for mesh independence study ranges from 2 to 6.1 million.

3. Results and Discussions

This section provides a comparison of the thermal-hydraulic characteristics of various lattices at different Reynolds numbers, ranging from 600 to 2000. The Reynolds number is determined using Eqs. (1) and (2), where ρ denotes fluid density of fluid, V represents the inlet velocity, D_h stands for hydraulic diameter, and μ signifies the fluid's viscosity.

$$Re = \frac{\rho V D_h}{\mu} \tag{1}$$

$$D_h = \frac{4(Total\ Fluid\ Volume)}{Total\ Fluid\ to\ Solid\ Surface\ Area} \tag{2}$$

3.1. Heat Transfer

Figure 3 presents a comparison of heat transfer among different lattices. The results indicate that the TYPE-D lattice exhibits the highest heat transfer, followed by TYPE-A lattice. Furthermore, all the lattices outperform the SC-BCC lattice. TYPE-B, TYPE-C, and TYPE-D lattices share the same structure but have different porosities, revealing that as porosity decreases, fluid mixing improves, leading to enhanced heat transfer.

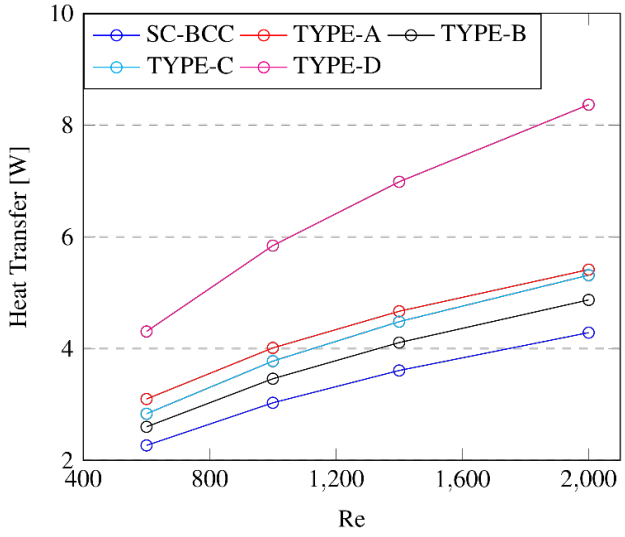

Fig. 3: Heat Transfer Comparison of different lattices at different Re.

Equation (3) provides the expression for total heat transfer, which depends on three factors: overall heat transfer coefficient (U), total heat transfer area (A_{total}) and LMTD. However, LMTD is primarily governed by inlet and plate temperatures. Hence, the significant parameters impacting heat transfer are overall heat transfer coefficient and total heat transfer area.

$$Q = UA_{total}(LMTD) \tag{3}$$

Table 1 presents a comparison of the total heat transfer areas of different lattices. Despite having a higher porosity TYPE-D lattice, TYPE-A lattice exhibits a comparable total heat transfer area. Moreover, since TYPE-B, TYPE-C, and TYPE-D lattices are structurally identical but differ in porosity, it can be concluded that reducing porosity leads to an in the total heat transfer area.

Table 1: Total Area comparison of different lattices.

Lattice	Total Heat Transfer Area (mm^2)	Plate Heat Transfer Area (mm^2)	Lattice Heat Transfer Area (mm^2)
SC-BCC	415.059	55.505	359.554
TYPE-A	597.699	70.973	526.726
TYPE-B	511.833	52.585	460.728
TYPE-C	531.116	50.408	480.708
TYPE-D	601.088	39.436	561.652

Equation (4) expresses the overall heat transfer coefficient, which depends mainly on heat transfer coefficient of the plate (h_{plate}) and lattice ($h_{lattice}$), heat transfer area of the plate (A_{plate}) and lattice ($A_{lattice}$), total heat transfer area, and fin efficiency (η).

$$U = \frac{h_{plate}A_{plate} + \eta h_{lattice}A_{lattice}}{A_{total}} \tag{4}$$

Numerical simulations can provide heat transfer values from the plate and lattice to the fluid. Therefore, one approach to compute heat transfer coefficient and fin efficiency involves using Eqs. (5) and (6). Here, we assume that h_{plate} and $h_{lattice}$ are equivalent to h, resulting in a single heat transfer coefficient throughout the domain. Q_{plate_fluid} and $Q_{lattice\_fluid}$ refer to heat transfer from the plate and lattice to the fluid, respectively. However, this method results in a fin efficiency greater than 100% for SC-BCC lattice at Reynolds number 600, indicating that the heat transfer coefficients for the plate and lattice sides are distinct.

$$Q_{plate\_fluid} = hA_{plate\_fluid}(LMTD) \tag{5}$$

$$Q_{lattice\_fluid} = \eta hA_{lattice\_fluid}(LMTD) \tag{6}$$

To compute the heat transfer coefficient for the plate and lattice sides, Eq. (7) and Eq. (8) are applied at every cross-section along the flow at intervals of 0.25 mm. Then, the volumetric average of the heat transfer coefficient is determined by taking the average over the length of the plate and lattice. At each cross-section, $q''_{plate\_fluid}(x)$ and $q''_{lattice\_fluid}(x)$ denote the heat flux from the plate and lattice, respectively, while $T_{plate}(x)$ and $T_{lattice}(x)$ indicate the average temperature of the plate and lattice, respectively. Additionally, $T_{BMT}(x)$ is the bulk mean temperature at that particular cross-section. To verify the calculation process, the heat transfer coefficient obtained using this method on the plate side is compared to the heat transfer coefficient obtained using Eq. (5), and the results are found to be almost identical. Then Eq. (6) can be used with lattice heat transfer coefficient to calculate fin efficiency.

$$h_{plate\_fluid} = \frac{q''_{plate\_fluid}(x)}{T_{plate}(x) - T_{BMT}(x)} \tag{7}$$

$$h_{lattice\_fluid} = \frac{q''_{lattice\_fluid}(x)}{T_{lattice}(x) - T_{BMT}(x)} \tag{8}$$

Figure 4a compares the plate heat transfer coefficients for different lattices. As it depicts, plate heat transfer coefficient is highest for TYPE-D lattice because the plate heat transfer coefficient follows flow over a flat plate trend, and the TYPE-D lattice has the highest inlet velocity. TYPE-D lattice has the least hydraulic diameter due to its high total heat transfer area and less fluid flow volume, so to maintain the same Reynolds number inlet velocity of the TYPE-D lattice has to increase. The lattice heat transfer coefficient comparison of different lattices at different Reynolds numbers is shown in Fig. 4b. TYPE-A lattice shows a superior lattice heat transfer coefficient because of the proper mixing of the fluid in every cross-section.

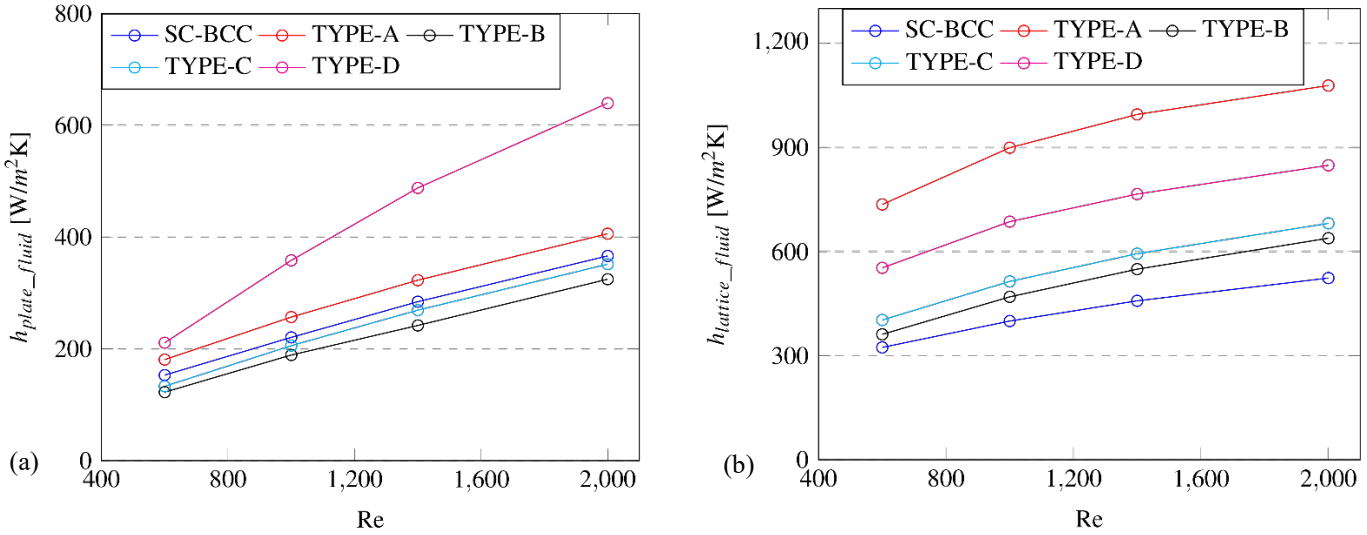

Fig. 4: (a) Plate heat transfer coefficient (b) Lattice heat transfer coefficient Comparison of different lattices at different Re

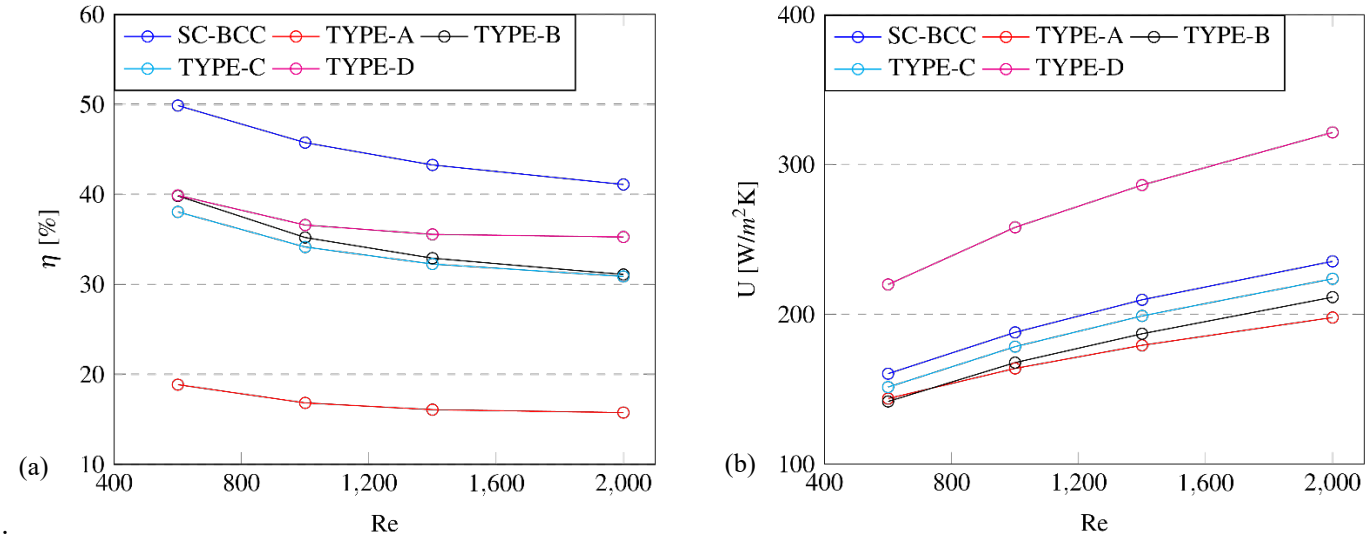

Fig. 5: (a) Fin efficiency and (b) Overall Heat Transfer Coefficient Comparison of different lattices at different Re.

Table 1 displays the heat transfer areas of the plate and lattice, which reveals that TYPE-D lattice has the highest lattice heat transfer area, whereas TYPE-A lattice has the highest plate heat transfer area. As shown in Fig. 1b, TYPE-A lattice has a smaller base area, resulting in the maximum plate heat transfer area. On the other hand, TYPE-D lattice has the least porosity, resulting in the maximum lattice heat transfer surface area.

The comparison of fin efficiency for various lattices is illustrated in Fig. 5a. Among all the lattices, TYPE-A lattice has the lowest fin efficiency. Due to this reason, despite having the highest lattice heat transfer coefficient and second highest lattice heat transfer area, it has almost 32.489% less heat transfer than TYPE-D lattice. Also, TYPE-B, TYPE-C and TYPE-D lattices are identical with different strut diameters, and from the graph, it can be concluded that fin efficiency depends on strut diameter. Despite having same strut diameter as SC-BCC lattice, TYPE-D lattice has different fin efficiency. Same can be concluded from TYPE-A and TYPE-B lattices. From this, it is clear that fin efficiency depends both on lattice structure and strut diameter.

The preceding discussion focuses on the combined impact of various parameters on the overall heat transfer coefficient. Fig. 5b depicts a comparison of the overall heat transfer coefficients of the different lattices at different Reynolds numbers. It can be concluded from the graph that the overall heat transfer coefficient of the TYPE-A lattice is the lowest due to its lower fin efficiency. Furthermore, only TYPE-D lattice has a higher overall heat transfer coefficient than the SC-BCC lattice structure.

3.2. Pressure Drop

Figure 6 compares the pressure drop (ΔP) among different lattices. The increased pressure drop in the TYPE-D lattice is a result of its higher inlet velocity, which is required to maintain the same Reynolds number. Additionally, all lattices exhibit higher pressure drops than the SC-BCC lattice due to their complex structure. TYPE-B lattice, a modified version of TYPE-A lattice with the same strut diameter, is designed to reduce pressure drop than TYPE-A lattice. The graph depicts that TYPE-B lattice achieve less pressure drop than TYPE-A lattice.

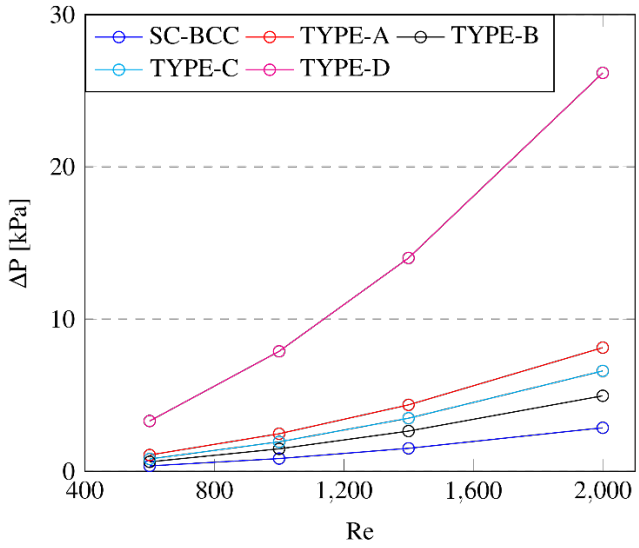

Fig. 6: Pressure drop Comparison of different lattices at different Re.

3.3. Area Goodness Factor

Figures 3 and Fig. 6 indicate that the heat transfer and pressure drop trends are closely related. Lattices with higher heat transfer also exhibit higher pressure drop. Therefore, to compare different lattices based on their thermal-hydraulic behaviour, area goodness factor is calculated. The area goodness factor is the ratio of the Colburn j-factor to the fanning friction factor as represented by Eq. (11). The formulas for Colburn j-factor and fanning friction factor are given by Eq.

(9) and (10), respectively. Here, Nu is Nusselt Number, Pr is Prandlt number, L is the length of the domain, ρ is the density of the fluid, A_{inlet} is the inlet area, G is mass flux, $\dot{m}$ is the mass flow rate and φ is porosity.

$$Colburn\,J-Factor\,(j)=\frac{Nu}{RePr^{\frac{1}{3}}} \tag{9}$$

$$Friction\,Factor\,(f)=\frac{\Delta P}{L}\left(\frac{\rho D_h}{2G^2}\right) \qquad G=\frac{\dot{m}}{\varphi A_{inlet}} \tag{10}$$

$$Area\,Goodness\,Factor=\frac{j}{f} \tag{11}$$

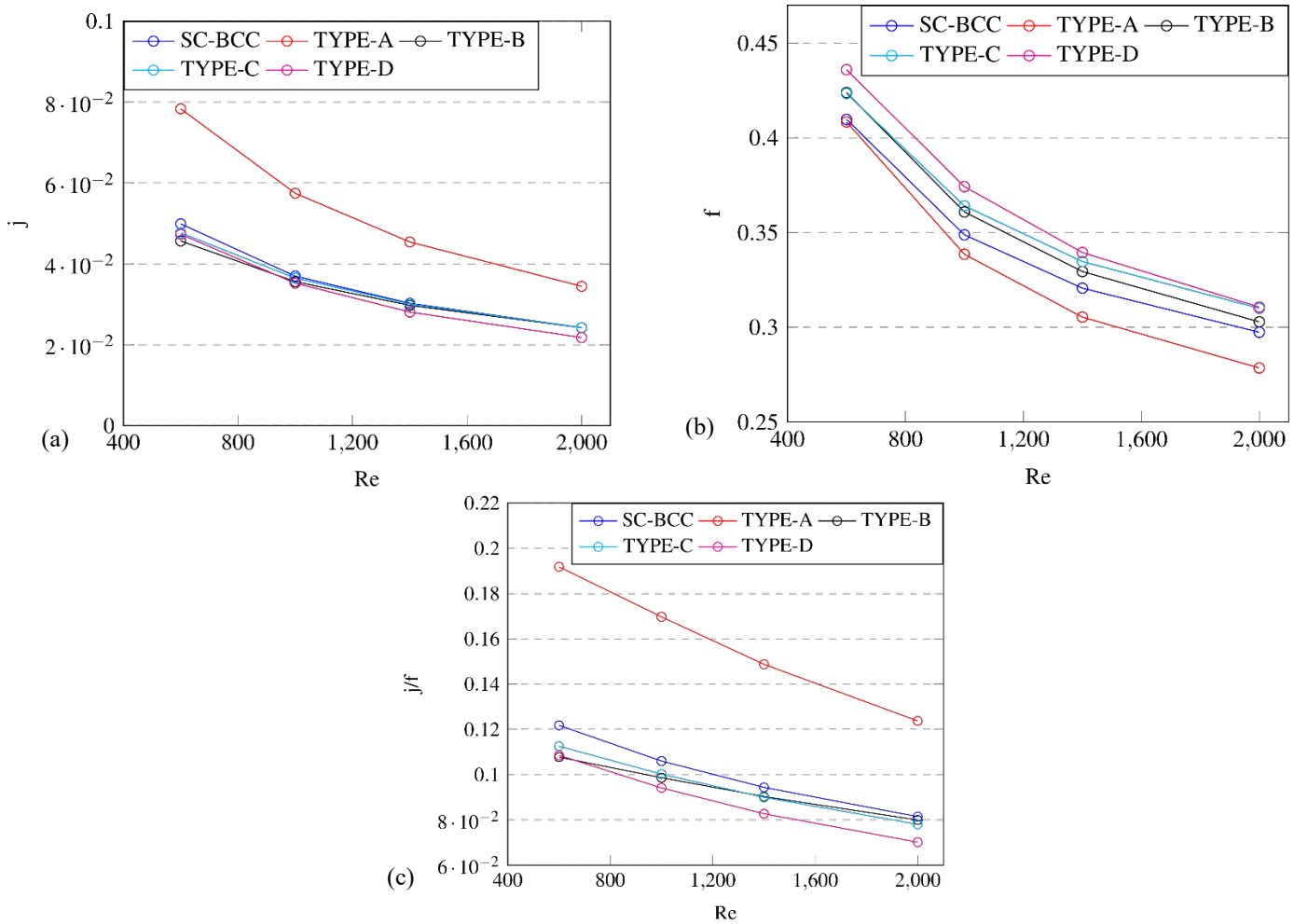

Fig. 7: (a) Colburn j-Factor, (b) Friction Factor and (c) Area Goodness Factor Comparison of different lattices at different Re.

The Colburn j-factor is calculated using the lattice heat transfer coefficient, and since Re and Pr are constant for every lattice, the variation in the Colburn j-factor is solely due to Nu. As depicted in Fig. 7a, the TYPE-A lattice has the highest Colburn j-factor due to its higher lattice heat transfer coefficient. Despite having the second-highest lattice heat transfer coefficient, TYPE-D lattice exhibits a lower Nu due to its lower hydraulic diameter, resulting in a lower Colburn j-factor.

The graph presented in Fig. 7b indicates that TYPE-D lattice has the highest friction factor compared to other lattices. The increased friction factor in TYPE-D is due to the combined effect of pressure drop, hydraulic diameter, and velocity.

Although TYPE-A lattice has the second highest pressure drop, because of its smaller hydraulic diameter and higher mass flow rate, it has a lower friction factor than all other lattices.

Figure 7c illustrates a comparison of the area goodness factor among all lattices at different Reynolds numbers. This graph indicates that TYPE-A lattice has the highest area goodness factor because of its higher lattice heat transfer and lower friction factor compared to other lattices. TYPE-A lattice exhibits the best thermal-hydraulic behaviour among lattices and demonstrates almost a 50% higher area goodness factor than SC-BCC lattice. On the other hand, other lattices have lower area goodness factors than SC-BCC lattice. Despite having the highest heat transfer among all lattices, TYPE-D lattice has the lowest area goodness factor due to its higher pressure drop, indicating the worst thermal-hydraulic behaviour.

4. Conclusion

The study examines the thermal-hydraulic behaviour of two new lattice structures with different strut diameters and compares them with the conventional SC-BCC lattice structure for various Reynolds numbers. It is observed from the results that heat transfer coefficient is different for the plate and lattice sides. Also, all the lattices show superior thermal performance than SC-BCC lattice, but SC-BCC has superior hydraulic performance. Due to higher inlet velocity, TYPE-D lattice has highest plate heat transfer coefficient. TYPE-A lattice has the highest lattice heat transfer coefficient, but due to less fin efficiency, it has less overall heat transfer coefficient. It is also observed that fin efficiency of lattices depends on both lattice geometry and strut diameter.

TYPE-D lattice has the highest pressure drop, followed by TYPE-A lattice. The reason for higher pressure drop of TYPE-D lattice is less porosity. TYPE-B lattice, which is a modified version of TYPE-A lattice, shows less pressure drop than TYPE-A lattice, although both have same diameter.

Finally, area goodness factor is checked for each lattice to find a lattice with the best thermal-hydraulic behaviour. TYPE-A has the highest area goodness factor. Only TYPE-A lattice shows superior performance than SC-BCC lattice, with 50% more area goodness factor than SC-BCC lattice. Due to higher pressure drop, despite having highest heat transfer, area goodness factor of TYPE-D lattice is very less.

References

[1] T. Dixit, P. Nithiarasu, and S. Kumar, “Numerical evaluation of additively manufactured lattice architectures for heat sink applications,” *Int. J. Therm. Sci.*, vol. 159, p. 106607, 2021.

[2] S. Takarazawa, K. Ushijima, R. Fleischhauer, J. Kato, K. Terada, W.J. Cantwell, S. Hasumoto, "Heat-transfer and pressure drop characteristics of micro-lattice materials fabricated by selective laser metal melting technology," *Heat Mass Transf.* vol. 58, pp. 125–141, 2022.

[3] S. Yun, J. Kwon, D. C. Lee, H. H. Shin, and Y. Kim, “Heat transfer and stress characteristics of additive manufactured FCCZ lattice channel using thermal fluid-structure interaction model,” *Int. J. Heat Mass Transf.*, vol. 149, p. 119187, 2020.

[4] M. Wong, I. Owen, C. J. Sutcliffe, and A. Puri, “Convective heat transfer and pressure losses across novel heat sinks fabricated by Selective Laser Melting,” *Int. J. Heat Mass Transf.*, vol. 52, no. 1–2, pp. 281–288, 2009.

[5] D. Liang, G. He, W. Chen, Y. Chen, and M. K. Chyu, “Fluid flow and heat transfer performance for micro-lattice structures fabricated by Selective Laser Melting,” *Int. J. Therm. Sci.*, vol. 172, Part B, p. 107312, 2022.

[6] V. Kumar, G. Manogharan, and D. R. Cormier, “Design of periodic cellular structures for heat exchanger applications,” *Proceedings of the 20th annual international solid freeform fabrication symposium (SFF’2009),* Austin, TX, August 2009, pp.738–748.

[7] X. Shi, Z. Yang, W. Chen, and M. K. Chyu, “Investigation of the effect of lattice structure on the fluid flow and heat transfer of supercritical CO2 in tubes,” *Appl. Therm. Eng.*, vol. 207, p. 118132, 2022.